***Representing nighttime and minimum conductance in CLM4.5: Global hydrology and carbon sensitivity analysis using observational constraints***

Lombardozzi, D.L.[1*], Zeppel, M.J.B [2], Fisher, R.A[1]. Tawfik, A.[1,3]

[1]National Center for Atmospheric Research, Boulder, CO, USA

[2]Department of Biological Sciences,
Macquarie University, Sydney, Australia.

[3]Center for Ocean-Land-Atmosphere Studies
George Mason University, Fairfax, VA, USA

[*] Corresponding author email: dll@ucar.edu

**Abstract**

The terrestrial biosphere regulates climate through carbon, water, and energy exchanges with the atmosphere. Land surface models estimate plant transpiration, which is actively regulated by stomatal pores, and provide projections essential for understanding Earth's carbon and water resources. Empirical evidence from 204 species suggests that significant amounts of water are lost through leaves at night, though land surface models typically reduce stomatal conductance to nearly zero at night. Here, we test the sensitivity of carbon and water budgets in a global land surface model, the Community Land Model (CLM) version 4.5, to three different methods of incorporating observed nighttime stomatal conductance values. We find that our modifications increase transpiration up to 5% globally, reduce modeled available soil moisture by up to 50% in semi-arid regions, and increase the importance of the land surface in modulating energy fluxes. Carbon gain declines up to ~4% globally and >25% in semi-arid regions. We advocate for realistic constraints of minimum stomatal conductance in future climate simulations, and widespread field observations to improve parameterizations.

## 1. Introduction

Terrestrial plants must balance their need to obtain $CO_2$ with the risk of desiccation if transpiration continues unchecked. Higher plants evolved stomatal pores to control the exchange of water and carbon between the leaf interior and the atmosphere (Hetherington and Woodward, 2003). Stomatal function, thus, is the dominant control over terrestrial fluxes of water and carbon. Most large-scale land-surface models use an empirical representation of stomatal

conductance ($g_s$), similar to the Ball-Woodrow-Berry (BWB) model (Ball, 1988; Ball et al., 1987; Collatz et al., 1991; Leuning, 1995; Medlyn et al., 2011; Sellers et al., 1996), to calculate plant gas exchange. The BWB model is linear, with two constants, the intercept ($g_o$) and slope ($g_1$), and estimates $g_s$ from the rate of $CO_2$ assimilation ($A$), atmospheric humidity ($h_r$), and internal leaf $CO_2$ concentration. The original BWB model parameters were fitted to observations of leaf gas exchange for ten plant species, with different $g_o$ values for each species, ranging from -310 to 130 mmol $m^{-2}$ $s^{-1}$ (Ball, 1988). The Community Land Model (CLM), however, uses only two $g_o$ values, (10 and 40 mmol $m^{-2}$ $s^{-1}$ for $C_3$ plants and $C_4$ plants, respectively; Collatz et al., 1991; Oleson et al., 2013; Sellers et al., 1996). Conductance during the night (and at other times when $A$ is 0) is thus represented using $g_o$. Recent advances in our ability to observe nighttime stomatal conductance (Caird et al., 2007; Phillips et al., 2010), $g_{s,n}$, illustrate that values are often larger in the field than the BWB parameters used in the CLM.

A comprehensive database (see Table S1) of 204 observed $g_{s,n}$ values illustrates that the minimum BWB $g_s$ values (equivalent to $g_o$) used in the CLM starkly differ with observed mean and median $g_{s,n}$ values. The available data for $g_{s,n}$ range from 0-450 mmol $m^{-2}$ $s^{-1}$ with an overall mean of 78 mmol $m^{-2}$ $s^{-1}$ (excluding hemi-parasites and CAM plants, which were omitted from model testing). Observations of $g_{s,n}$ are, on average, ten times higher in broadleaf tropical deciduous species (Table 1; 129 mmol $m^{-2}$ $s^{-1}$) and seven times higher in temperate broadleaf deciduous trees (73 mmol $m^{-2}$ $s^{-1}$) compared to the 10 mmol $m^{-2}$ $s^{-1}$ used for $C_3$ plants. Potential benefits of a high $g_{s,n}$ might include the transport of nutrients (Dios et al., 2013; Scholz et al., 2007; Zeppel et al., 2014) or processes related to embolism repair, phloem transport, or xylem refilling that

might improve carbon gain, but these ideas remain untested. Nonetheless, the discrepancy between parameterized $g_o$ and observed $g_{s,n}$ serves as motivation to investigate the sensitivity of simulated land surface processes to more realistic minimum $g_s$ values. Such field measurements of $g_{s,n}$ have not previously been incorporated into a global land surface model, despite the possible impacts on surface hydrology, ecosystem carbon gain, and land-atmosphere feedbacks.

We use a global land-surface model, the Community Land Model (CLM) version 4.5, forced with a data atmosphere and driven with observed ('satellite phenology') leaf area indices (CLM4.5SP), to test the sensitivity of the land surface to using realistic minimum $g_s$ from observed $g_{s,n}$, averaged by plant functional type (PFT; Table 1). Since the BWB approach is primarily intended to predict daytime stomatal behavior, the appropriate method for application of observed $g_{s,n}$ within the context of the BWB model is unclear. We therefore test three methodologies for implementing observed $g_{s,n}$: 1) modifying the BWB intercept ($g_o$); 2) setting a nighttime threshold value; and 3) setting a minimum threshold value. We anticipate that implementing observed $g_{s,n}$ values will increase plant transpiration, altering carbon and water budgets on regional and global scales.

## 2. Methods

### *2.1 Model Description and Simulation Design*

The CLM4.5SP model used here is an updated version of CLM4.0, originally described by Lawrence et al., (2011), with updated technical details for v4.5 described by Oleson et al., (2013). The CLM4.5SP simulations were run with

CRU-NCEP climate forcing data (combines Climate Research Unit (CRU) TS 3.2 monthly climatology with National Oceanic and Atmospheric Administration National Center for Environmental Prediction (NCEP) and NCAR 2.5° x 2.5° 6-hourly reanalysis; (downloaded at: http://dods.ipsl.jussieu.fr/igcmg/IGCM/BC/OOL/OL/CRU-NCEP/), a historical atmospheric dataset that includes observed precipitation, temperature, downward solar radiation, surface wind speed, specific humidity, and air pressure from 1901 through 2010, and did not include the influences of nitrogen deposition, land use change, or changing $CO_2$ concentrations.

The CLM4.5SP uses the coupled Farquhar photosynthesis and BWB $g_s$ models to simulate plant physiology (Bonan et al., 2011; Oleson et al., 2013). The BWB $g_s$ is calculated based on the equation:

$$g_s = g_0 * \beta_{soil} + g_1(Ah_r/C_a) \quad (Eq.\ 1)$$

where $g_0$ and $g_1$ are empirical fitting parameters of the minimum $g_s$ and the slope of the conductance-photosynthesis relationship, respectively; $A$ is net carbon assimilation rate (μmol C $m^{-2}$ $s^{-1}$); $h_r$ is the fractional humidity at the leaf surface (dimensionless), $C_a$ is the $CO_2$ concentration at the leaf surface (μmol $mol^{-1}$), and $\beta_{soil}$ is the soil wetness scalar, ranging from zero to one (see Oleson et al. 2013). $\beta_{soil}$ is calculated as:

$$\beta_{soil} = \Sigma_i\, w_i r_i \quad (Eq.\ 2)$$

where $w_i$ is a plant wilting factor for layer $i$ and $r_i$ is the fraction of roots in layer $i$. When implemented in the unmodified CLM4.5SP, $g_0$ is 10 mmol $m^{-2}$ $s^{-1}$ for all $C_3$ plants and 40 mmol $m^{-2}$ $s^{-1}$ for all $C_4$ plants, and is adjusted by $\beta_{soil}$ (varying from 0-1) every time-step. It is also important to note that $\beta_{soil}$ is also applied to the

115 $V_{c,max}$ (the maximum rate of carboxylation) parameter in the *A* equation, as well
116 as to leaf maintenance respiration (Oleson et al. 2013).
117 Values of $g_{s,n}$ based on literature data (Table S1) are typically larger than
118 the $g_0$ values used in current implementations of the BWB model. The $g_{s,n}$ data,
119 grouped and then averaged by PFT (Table 1), were used to modify simulated
120 minimum $g_s$ using three methodologies. First, the '$\Delta g_0$' method replaced the BWB
121 minimum conductance, $g_0$, value for each PFT with the observed $g_{s,n}$ (Table 1),
122 resulting in a uniform increase to $g_s$ during both day and night (referred to as the
123 $\Delta g_o$ simulation; tested previously by Barnard and Bauerle, 2013). Second, the
124 $\Delta g_{night}$ method implemented the BWB model in its standard form (Eq. 1; the $g_o$
125 and $g_1$ values are the same as the control), but included a minimum threshold
126 that was applied only at night, based on observed $g_{s,n}$ for each PFT, below which
127 $g_s$ could not fall. In the $\Delta g_{night}$ simulation, daytime $\Delta g_s$ occasionally fell below the
128 observed nighttime threshold on account of high vapor pressure deficit (VPD) or
129 low assimilation rates. To avoid this potentially unrealistic behavior, we use a
130 third method, '$\Delta g_{min}$', which extended the observation-based threshold used in
131 the $\Delta g_{night}$ simulation to all times during the day or night, so that $g_s$ never fell
132 below the minimum threshold value found in Table 1. These three modified
133 simulations were compared to a control simulation using the unmodified BWB
134 formulation. Similar to the unmodified and $\Delta g_o$ simulations that adjust the $g_o$
135 parameter based on a soil wetness scalar ($\beta_{soil}$), the $\Delta g_{night}$ and $\Delta g_{min}$
136 modifications also adjusted the minimum $g_s$ threshold by $\beta_{soil}$ at every time-step.
137 Each simulation was run for 25 years with monthly output to determine the

138 long-term impact of changing minimum conductance, and for one year with half-
139 hourly output to determine the changes in diel patterns.
140
141 *2.2 Data Collection*
142 Values of $g_{s,n}$ were obtained from field and glasshouse studies, using
143 Scopus (www.scopus.com), with data for 204 records across 150 species and
144 cultivars (Table S1). Records available were predominately for temperate plants
145 (93 records) and crops (34), with more data available for broad-leaf plant types
146 (89) than needle-leaf plants (16; Zeppel et al., 2014). The data were collated by
147 plant functional type (PFT), with means, medians, and standard deviations for
148 each PFT presented in Table 1. Simulations presented here were run with mean
149 values for each PFT, though median values were also tested and are presented in
150 SI Figure 3 and SI Figure 4. Since there is large variability in the PFT responses,
151 we present the range of variability in SI Figure 2.
152 The measurements of each $g_{s,n}$ value are generally obtained from steady
153 state porometers, diffusion porometers, Licor 1600 and Licor 6400 gas exchange
154 systems (Caird et al., 2007; Phillips et al., 2010), with a small number converted
155 from sap flux (Benyon 1999) using an inverted Penman-Monteith equation.
156 Different sampling methods may lead to different estimates of $g_{s,n}$, and
157 measureable $g_{s,n}$ typically only occurs where VPD is above zero. For example,
158 using a cuvette clamped over the leaf, which changes the leaf boundary layers,
159 will be different compared to measurements from sap flow with an unaltered
160 boundary layer. Data for $g_{s,n}$ were typically reported during well-watered
161 conditions, which is ideal because the CLM4.5 calculates stomatal $g_s$ without

water stress and then adjusts $g_o$ values (and modifications additionally adjust $g_{night}$ and $g_{min}$ thresholds) using a soil wetness scalar.

*2.3 Terrestrial Coupling Index*

To investigate the impact of stomatal conductance changes on the atmosphere, a terrestrial coupling index was calculated, allowing examination of the influence of a minimum $g_s$ threshold on land-atmosphere coupling. Following Dirmeyer (2011), the terrestrial segment of land-atmosphere coupling is defined as:

$$\text{Terrestrial Coupling Index (TCI)} = \sigma_w * \beta_{w,ET} \qquad \textit{(Eq. 3)}$$

where $\sigma_w$ is the standard deviation of root-zone soil moisture relevant for transpiration across a given season (e.g., 25 years times 3 summer months), and $\beta_{w,ET}$ is the linear slope of monthly mean evapotranspiration and root-zone soil moisture. The TCI captures the variability ($\sigma_w$) and sensitivity of evapotranspiration to changes in soil moisture and returns units equivalent to those of evapotranspiration. Therefore, for a region to have high TCI, soil moisture must have high variability thus enabling any evapotranspiration-soil moisture sensitivity to manifest in the climate system. While this is strictly a metric for defining the terrestrial component of coupling, the terrestrial component has been used as a surrogate for the total soil moisture-precipitation coupling pattern because of the strong spatial pattern correlation (Wei and Dirmeyer, 2012).

## 3. Results and Discussion

### *3.1 Implementation of $g_{s,n}$*

Incorporating observed minimum constraints on $g_s$ in all modified simulations increased $g_s$ and transpiration compared to the control simulation, illustrated in Fig. 1 for a highly impacted semi-arid location in Ethiopia (see Fig. S1 for other regions). The large variability in the observational dataset causes substantial uncertainty in the simulations, masking the differences among parameterizations and highlighting the impact of $g_{s,n}$ on transpiration (Fig. S2). The sensitivity of $g_s$ and transpiration to the altered $g_o$ parameter in the $\Delta g_o$ simulation is large (Barnard and Bauerle, 2013; Bowden and Bauerle, 2008). Since the higher $g_o$ is added to $g_s$ in the BWB calculation at every model time step (see Eq. 1), altering $g_o$ increases transpiration throughout the entire diel cycle, and produces changes in the daytime evaporative flux that are not supported by observations of $g_{s,n}$. We consider that uniformly adjusting the $g_o$ parameter does not represent the correct implementation of observed $g_{s,n}$ values.

If $g_o$ cannot be equated to plant minimum $g_s$ in the BWB paradigm, this raises the possibility of whether $g_o$ has a theoretical interpretation beyond an empirical fitting parameter. It is possible that $g_o$ is equivalent to cuticular conductance ($g_{cut}$), or conductance that is not regulated by the stomatal guard cells (Caird et al., 2007), occurring during the day and night. Niyogi and Raman (1997) describe $g_o$ as cuticular conductance, though there is no record of $g_o$ being tested or described as $g_{cut}$ previously. Studies that have quantified $g_{cut}$ found that $g_{cut}$ was a low proportion, < 10%, of total $g_s$ and less than measured $g_{s,n}$ (Caird et al., 2007; Zeppel et al., 2014). The values of $g_o$ used in current implementations of the Ball-Berry model for $C_3$ plants (10 mmol $m^{-2}$ $s^{-1}$) fall

within the range of measured $g_{cut}$ values (4 to 20 mmol $m^{-2}$ $s^{-1}$; Caird et al., 2007). Assuming $g_o$ does have a theoretical function of representing $g_{cut}$, rather than $g_{s,n}$, incorporating an observed threshold of minimum $g_s$ is necessary. Whether $g_o$ functions theoretically as $g_{cut}$ in the BWB model needs further evaluation, as adjusting simulated $g_o$ has large impacts on canopy conductance and transpiration (Fig 1; Barnard and Bauerle, 2013). Regardless, observed $g_{s,n}$ is larger than modeled $g_o$ and functions differently, and therefore should be considered independently in model parameterizations.

The $\Delta g_{min}$ and $\Delta g_{night}$ simulations represent the intended change in minimum $g_s$ with greater fidelity, by limiting the minimum value without increasing $g_s$ at every model time step. Interestingly, in restricting only nighttime conductance, the $\Delta g_{night}$ simulation allows daytime $g_s$ to decrease below the nighttime threshold during the dry season in semi-arid ecosystems (Fig. 1a). This occurs when $A_n$ nears zero in shade or low humidity, causing $g_s$ to fall to the default (lower) $g_o$. In contrast, the $\Delta g_{min}$ simulation restricts minimum $g_s$ at all times, and therefore daytime values are never less than the water-adjusted $g_{s,n}$. This increases canopy-averaged daytime $g_s$, and hence transpiration, compared to the unmodified simulation whenever daytime $g_s$ values fall below the minimum threshold (Fig. 1a, c).

The data in Table S1 is a compilation of all available published $g_{s,n}$ data to date, and reports $g_{s,n}$ values for 204 distinct plants. Of these, only four plants exhibit higher $g_{s,n}$ than daytime $g_s$, and two of those are Crassulacean acid metabolism (CAM) plants, which by definition open their stomata at night to gain carbon dioxide and close their stomata during the day, and were not used in our parameterization. These data suggest that, as expected, $g_{s,n}$ is typically less than

daytime $g_s$. Most data presented in Table S1 are average values under non-drought stressed conditions, and are likely only reported for leaves in sunlit canopy layers. Thus, these data do not elucidate whether, at any given time, daytime values might drop below the nighttime threshold, but only suggest that, on average, they do not.

In the context of the model simulations, low daytime $g_s$ occurs any time that $Ah_r/C$ is low. These are conditions which are poorly illuminated (in shade or at dawn/dusk and night), or when humidity is low. The CLM4.5SP contains a representation of the shaded canopy, which has lower $g_s$ and often reaches the minimum daytime threshold ($g_o$ in the unmodified, $\Delta g_o$, and $\Delta g_{night}$ simulations; and $g_{s,n}$ in the $\Delta g_{min}$ simulation). The central issue in determining whether the $\Delta g_{min}$ or $\Delta g_{night}$ simulation is a better representation of minimum $g_s$ is whether, under the same conditions in the real world, daytime $g_s$ might be lower than $g_{s,n}$. For example, if observational data support that daytime $g_s$ is less than $g_{s,n}$ in shaded canopy layers given the same water availability, then the $\Delta g_{night}$ simulation is a better parameterization. However, if observational data suggest that daytime $g_s$ is consistently higher than $g_{s,n}$, then the $\Delta g_{min}$ simulation is a better parameterization. While observational data are not available to specifically answer this question, the available data presented in Table S1 and data from Dawson et al. (2007), which suggest that $g_{s,n}$ is a fraction of daytime $g_s$, imply that daytime $g_s$ is on average higher than $g_{s,n}$, providing partial support for the $\Delta g_{min}$ implementation. A different implementation of $g_{s,n}$ might calculate $g_{s,n}$ as a proportion of daytime $g_s$, based on Dawson et al. (2007), who find that $g_{s,n}$ is a proportion of daytime $g_s$ that changes based on days since last rainfall. We do

261 not test this potential method here, but acknowledge it as a viable alternative to
262 be considered.

263 The possible existence of a higher $g_{s,n}$ compared to daytime $g_s$ raises an
264 interesting question about the potential selective advantage for leaves with a
265 high $g_{s,n}$. It is hypothesized that high $g_{s,n}$ may provide a beneficial function to the
266 plant, such as embolism repair or phloem transport (e.g., Dawson et al. 2007).
267 Additionally, $g_{s,n}$ may contribute to xylem refilling, potentially improving carbon
268 gain by making water available when light conditions allow for photosynthesis
269 (Dawson et al. 2007). Critically, it is not clear whether these potential functions
270 are only relevant at night (and daytime $g_s$ can be lower than $g_{s,n}$), or whether
271 high $g_{s,n}$ is representative of a general strategy of higher overall minimum $g_s$. We
272 are not aware of data that exist to support either possibility, and advocate for
273 observations that will help determine the functional significance of $g_{s,n}$.

274 From a model or theoretical perspective, it is important to note that the
275 reason that simulated $g_s$ values are reduced to as low as 10 mmol $m^{-2}$ $s^{-1}$ (or
276 lower, if down-regulated for water stress) is a function of the universal
277 parameterization of all $C_3$ plants with that value of $g_o$. Given that it is unlikely
278 that this value is universal for all plants, we consider that the large difference
279 between the $\Delta g_{min}$ or $\Delta g_{night}$ simulations is an artifact of the poorly constrained
280 parameterization of the daytime BWB model.

281 It should be noted that all the minimum thresholds implemented in our
282 simulations ($\Delta g_o$, $\Delta g_{night}$, and $\Delta g_{min}$) are adjusted by a soil water scalar ($\beta_{soil}$).
283 Therefore, the nighttime ($\Delta g_{night}$) and the minimum ($\Delta g_{min}$) thresholds are

altered according to the degree of soil moisture stress. When the daytime $g_s$ value is lower than the $g_{night}$ threshold in the $\Delta g_{night}$ simulation (Fig. 1c), the $g_{night}$ threshold is already down-regulated for water stress. In this scenario, the daytime minimum $g_s$ is less than the nighttime $g_s$ when water stress is equivalent.

Responses to dry soil conditions are mediated both through the minimum $g_s$ values, and through the impact of soil moisture on photosynthetic capacity and leaf maintenance respiration, which are also multiplied by $\beta_{soil.}$ Many of the impacts of our simulations result from feedbacks between higher transpiration rates resulting in faster depletion of soil moisture store, and therefore greater constraint on photosynthesis. These results are all emergent features of the model and should not be interpreted as direct results of the altered parameterization.

*3.2 Global Water and Carbon*

When averaged over 25 years, incorporating observed rates of $g_{s,n}$ in the $\Delta g_{min}$ simulation increased transpiration losses up to 30% in the Amazon, and >30% in some arid regions, in part due to the small absolute magnitude of available soil water (Fig. 2a-c). Semi-arid regions are primarily broad-leaf shrub and $C_3$ grass PFTs that have particularly high values (130 and 156 mmol $m^{-2}$ $s^{-1}$ respectively) of observed $g_{s,n}$ (Table 1), and have high nighttime vapor pressure deficits that interact with higher minimum $g_s$ values, causing large nighttime transpiration rates. Using median rather than mean values caused only small (<1.5%) differences in global transpiration (Fig. S3, Fig. S4). Though the magnitude of response is different depending on parameterization used, the

308 increases in transpiration imply that current model estimates of plant water loss
309 are underestimated in many regions.
310 Simulated higher transpiration resulting from higher minimum $g_s$ also has
311 ecosystem-scale ramifications for hydrology (McLaughlin et al., 2007). For
312 example, the increased transpiration resulted in drier soils compared to the
313 control simulation (Fig. 2g-i), with $\Delta g_{min}$ causing >40% soil moisture decreases in
314 semi-arid ecosystems like the Southwestern United States and much of Australia
315 (>10% in $\Delta g_{night}$). Additionally, the $\Delta g_{min}$ estimated changes to surface runoff are
316 large in some regions, such as the 10-25% decreases in the tropics (5-10% in
317 $\Delta g_{night}$; Fig. 2d-f), suggesting that current runoff estimates may be too large. It
318 should be noted that the difference between the $\Delta g_{min}$ and $\Delta g_{night}$ simulations is
319 largely due to changes in minimum $g_s$ that affect daytime $g_s$ (see Section 3.1).
320 Hydrologic changes in soil moisture and runoff in response to increased $g_s$ have
321 previously been documented in catchments in southeastern United States
322 (McLaughlin et al., 2007), and our results suggest that changes to stomatal
323 conductance have similar consequences in CLM4.5SP simulations. Additionally,
324 increasing minimum $g_s$ caused gross primary productivity (GPP) to decrease
325 (Figure 3) by 10 to >25% in many semi-arid regions. These are regions where
326 water availability already restricts GPP, and the decreases in soil moisture
327 caused by higher transpiration likely impart even more drought-induced
328 stomatal closure.
329 To more directly evaluate the potential influence of minimum $g_s$ on the
330 climate system, we calculate the change in terrestrial coupling to the
331 atmosphere. The terrestrial coupling index (Dirmeyer, 2011) estimates the
332 degree to which changes in soil moisture control surface energy fluxes to the

atmosphere. This study uses root-zone soil moisture rather than soil moisture over spatially constant soil depth to highlight the direct impact of vegetation and minimum $g_s$ on surface fluxes. Here we calculate the terrestrial coupling index during boreal summer months when warmer temperatures allow for the highest $g_s$ rates. We find that the terrestrial coupling strength increases when using the $\Delta g_{min}$ implementation, but is generally unchanged for $\Delta g_{night}$ (Fig. 4), meaning root-zone soil moisture exerts a greater control on surface flux variability for $\Delta g_{min}$, largely due to the impact this simulation has on daytime $g_s$. This increased terrestrial coupling to the atmosphere largely mirrors the reductions in GPP and soil moisture in semi-arid ecosystems, and may reinforce climate extremes such as droughts or heat waves (Hirschi et al., 2011; Miralles et al., 2014).

### *3.3 Evaluating $g_{s,n}$*

Evaluating the performance of the new $g_{s,n}$ parameterizations is challenging for numerous reasons. First, our model scales from leaf-level $g_s$ and $g_{s,n}$ estimates to canopy transpiration. The best way of evaluating the model is to compare simulated and observed canopy transpiration because the model captures the average of an entire canopy, which is comprised of multiple plant functional types, rather than individual plant functional types. Incorporating realistic minimum $g_s$ increases global evapotranspiration and decreases global runoff compared to globally-scaled observations, while estimates of GPP from all simulations fall within the range of global GPP estimates from observations (Table 2; Bonan et al., 2011, 2012; Li et al., 2011). However, these comparisons should be used with caution, since eddy covariance data used in estimating the GPP and evapotranspiration observations are susceptible to errors at night (Fisher et al., 2007; van Gorsel et al., 2008; Kirschbaum et al., 2007; Medlyn et al.,

358 2005) due to a lack of sufficient canopy turbulence that precludes detection of
359 nighttime transpiration using this measurement methodology, and are not useful
360 for evaluating the changes in water fluxes tested in this study. Other data for
361 evaluating model responses to minimum $g_s$ on large spatial scales are not yet
362 available.

363 A comparison of simulated canopy transpiration to transpiration
364 calculated from sap-flux data in Australia (Fig. 5) illustrates that a minimum $g_s$
365 threshold changes transpiration estimates during the early part of the night,
366 though simulated nighttime rates are still low compared to observations. All
367 model parameterizations fall within the observational range of uncertainty, but
368 under-predict nighttime and midday canopy transpiration during May and June,
369 and over-predict midday canopy transpiration in July. The lack of fidelity
370 between the various model parameterizations and the observations is likely
371 affected by the fact that observed meteorological data were unavailable to force
372 the model. Therefore, key parameters driving both daytime and nighttime
373 transpiration fluxes, such as VPD and soil water availability, were likely different
374 in the model simulations compared to the actual meteorological conditions at
375 Castlereagh during data collection. Additionally, because sap flow is measured at
376 the base of the tree, there is typically a lag between when sap flow is measured
377 and when the canopy transpires, and this lag is also notable in comparing
378 observed sap flow with simulated estimates of transpiration. Estimating
379 nighttime transpiration using sap flow methodology is also convoluted with the
380 refilling of aboveground water stores depleted during the day, and thus is not
381 directly comparable to our simulations. It should also be noted that the model

382 does not have a semi-arid plant functional type, so semi-arid plants are typically
383 represented in the model as deciduous plant functional types.
384 Given that our study focused only on one aspect of the $g_s$ formulation
385 within a land surface model, evaluating daytime $g_s$ and other aspects of the BWB
386 model function (i.e., photosynthetic drivers of daytime $g_s$, feedbacks to water
387 availability, etc.) are all subject to pre-existing deficiencies in the representation
388 of a host of other model processes. For example, there are only two values of the
389 $g_1$ (slope) parameter in the BWB model, one for $C_3$ and one for $C_4$ plants (Sellers
390 et al., 1996), and this parameter has not been modified or comprehensively
391 evaluated within the context of the CLM4.5SP. Indeed, the use of the BWB model
392 at all is currently the subject of some debate (Bonan et al., 2014; De Kauwe et al.,
393 2015), and this study additionally highlights how the empirical nature of the
394 BWB model leads to difficulties when attempting to implement mechanistic
395 processes. Further, daytime $g_s$ is also dependent on the photosynthetic capacity,
396 and observations of $V_{cmax}$ and $J_{max}$ (Bonan et al., 2011; Kattge and Knorr, 2007)
397 indicate very wide ranges of plant functional type variation in these properties,
398 also limiting our confidence that the globally averaged parameters used in the
399 default model will lead to accurate $g_s$ and transpiration at most locations. We
400 choose not to focus on these and other parameters that effect daytime $g_s$, as it
401 does not directly impact the representation of $g_{s,n}$, and is therefore beyond the
402 scope of this paper.
403
404 **4. Conclusion**
405 The rate of minimum $g_s$ estimated from the BWB model used in many
406 global land surface models is typically smaller than observed $g_{s,n}$ (Barnard and

Bauerle, 2013), as demonstrated in a review of 204 species (Zeppel et al., 2014). Including a nighttime or minimum $g_s$ threshold based on observations results in simulated hydrologic changes, such as decreased soil moisture and runoff (Fig. 2), particularly in semi-arid regions where water availability already restricts growth. In addition to potentially increasing drought stress in sensitive regions, this has the impact of reducing plant growth (Fig. 3) and changing the modeled terrestrial coupling to the atmosphere (Fig. 4). The difference between the $\Delta g_{min}$ and $\Delta g_{night}$ simulations highlights one outstanding uncertainty: Does minimum daytime $g_s$ decrease below nighttime $g_s$? While the balance of our arguments favors the $\Delta g_{min}$ implementation of $g_{s,n}$, this study primarily illustrates the potential sensitivity of global simulations to minimum $g_s$ considerations, and serves as motivation for additional field experiments, particularly in semi-arid areas, to discern better representations of low $g_s$ conditions during daytime and nighttime. To better understand the future of these sensitive ecosystems, widespread field observations, quantification of minimum daytime $g_s$, and a better understanding of the physiological causes and consequences of nighttime transpiration are necessary so that land surface models can robustly incorporate observations and theory.

## 5. Code and Data Availability

The code for CLM4.5 is publically available through Subversion code repository: https://svn-ccsm-models.cgd.ucar.edu/cesm1/release_tags/cesm1_2_2. To access the code, fill out a short, required registration to get a user name and password, necessary to gain access to the repository. http://www.cesm.ucar.edu/models/register/register_cesm.cgihttp://www.cesm.ucar.edu/models/cesm1.2/clm/CLM45_Tech_Note.pdf. The CLM4.5 User's

Guide can be found at:

http://www.cesm.ucar.edu/models/cesm1.2/clm/models/lnd/clm/doc/UsersGuide/book1.html. All stomatal conductance data used in developing the implementations can be found in Table S1.

## Author Contributions

DL, MZ, and RF conceived the project. MZ assembled the $g_{s,n}$ datasets; DL ran model simulations; and DL and AT analyzed model simulations, with guidance from RF. All authors contributed to writing the paper.


## Acknowledgements

We thank Gordon Bonan for useful discussion on the manuscript, and the reviewers for the constructive comments that have improved the final version of this paper. DL was supported through the DEB-Ecosystem Science cluster and National Science Foundations grant EF-1048481. MZ was supported by ARC DECRA DE120100518. RF was supported by the National Science Foundation and the National Center for Atmospheric Research, and AT was supported by the National Science Foundation grant 0947837 for Earth System Modeling post-doctoral fellows. The National Center for Atmospheric Research is funded by the National Science Foundation.

452 **Tables**

**Table 1**. Old and new minimum stomatal conductance values used in CLM4.5SP. Units are mmol $m^{-2}$ $s^{-1}$

| Plant Functional Type | Old Value | Mean New Value | Median New Value | Standard Deviation | n |
|---|---|---|---|---|---|
| temperate needle-leaf evergreen tree | 10 | 16.896 | 10 | 20.803 | 12 |
| boreal needle-leaf evergreen tree | 10 | 8 | 8 | NA | 1 |
| needle-leaf deciduous tree | 10 | 35.367 | 35 | 6.458 | 3 |
| tropical broadleaf evergreen tree | 10 | 90.488 | 75.5 | 67.850 | 8 |
| temperate broadleaf evergreen tree | 10 | 34.017 | 27 | 28.263 | 25 |
| tropical broadleaf deciduous tree | 10 | 129 | 129 | 41.012 | 2 |
| temperate broadleaf deciduous tree | 10 | 72.637 | 41.66 | 83.525 | 22 |
| boreal broadleaf deciduous tree | 10 | 50 | 50 | NA | 1 |
| broadleaf evergreen shrub | 10 | 65.353 | 29 | 116.062 | 16 |
| broadleaf deciduous shrub | 10 | 129.644 | 60 | 145.539 | 9 |
| c3 grass | 10 | 157.988 | 161 | 67.317 | 24 |
| C4 grass | 40 | 93.933 | 48.5 | 125.533 | 6 |
| crop | 10 | 60.629 | 36.7 | 60.745 | 21 |
| | | | | | 150 |

*New Value, Standard Deviation and n are based on data pooled from the literature.

453

454

455

**Table 2**. Global values from CLM simulations and observations[a]

| **Simulation** | **$g_{s,n}$ data used** | **GPP (Pg C $yr^{-1}$)** | **ET ($10^3$ $km^3$ $yr^{-1}$)** | **Runoff ($10^3$ $km^3$ $yr^{-1}$)** |
|---|---|---|---|---|
| Control | N/A | 157.83 | 65.6148 | 30.462 |
| $g_o$ | Mean | 152.56 | 72.6555 | 24.2141 |
| $g_{night}$ | Mean | 156.068 | 66.0926 | 30.0724 |
| $g_{min}$ | Mean | 151.252 | 68.6843 | 27.8161 |
| $g_o$ | Median | 153.641 | 71.5441 | 25.1739 |
| $g_{night}$ | Median | 156.346 | 66.031 | 30.119 |
| $g_{min}$ | Median | 152.385 | 67.8881 | 28.51 |
| Observation | | 119-175 | 65.13 | 37.7521 |

[a]Global gross primary productivity (GPP), evapotranspiration (ET) and runoff values. Observed values presented in Bonan et al. (2011), Welp et al. (2011), and Lawrence et al. (2011)

456

457

458 **Figure Captions**

459 **Figure 1.** Diurnal time-series of canopy conductance (a,c) and transpiration
460 (b,d) for Ethiopia over five days in mid-January (a-b) and mid-July (c-d). The
461 control simulation (solid black line) had lower conductance and transpiration
462 than the $\Delta g_o$ simulation (dotted red line) and the $\Delta g_{min}$ simulation (dashed blue
463 line). The $\Delta g_{night}$ simulation (dot-dashed teal line) had higher nighttime
464 conductance and transpiration than the control simulation, but similar daytime
465 conductance and transpiration, allowing for daytime conductance to fall below
466 the nighttime threshold. The $\Delta g_o$ simulation added the observed $g_{s,n}$ values to the
467 conductance calculation at every time, day or night, which is not theoretically
468 aligned with the function of including observed $g_{s,n}$. As a result, the $\Delta g_o$
469 simulation was eliminated from further analyses. Note that all minimum
470 thresholds ($g_o$, $g_{night}$, and $g_{min}$) were adjusted using a soil moisture scalar.

471

472 **Figure 2**. Simulated average transpiration (a), runoff (d), and soil moisture (g)
473 for a control simulation; and percent change from control in transpiration (b-c),
474 runoff (e-f), and soil moisture (h-i) after including a nighttime threshold ($\Delta g_{night}$;
475 b,e,h) or a minimum $g_s$ threshold ($\Delta g_{min}$; c,f,i) based on observational data. Note
476 that both nighttime and minimum thresholds were adjusted based on a soil
477 moisture scalar.

478

479 **Figure 3**. Average gross primary productivity (GPP) for a control simulation (a),
480 and percent change from control (b-c) after including a nighttime threshold
481 ($\Delta g_{night}$; b) or a minimum $g_s$ threshold ($\Delta g_{min}$; c) based on observational data.

Note that both nighttime and minimum thresholds were adjusted based on a soil moisture scalar.

**Figure 4**. Terrestrial coupling for June-July-August for a control simulation (a), and the difference from control (b-c) after including a nighttime threshold ($\Delta g_{night}$; b) or a minimum $g_s$ threshold value ($\Delta g_{min}$; c) based on observational data. Note that both nighttime and minimum thresholds were adjusted based on a soil moisture scalar.

**Figure 5.** Average diel canopy transpiration for the months of May, June, and July in Castlereagh, Australia (observation, dotted black line), estimated from sap flux measurements of Red Gum and Iron Bark, the dominant tree species in the canopy. Average simulated canopy transpiration for the grid cell corresponding to Castlereagh, Australia for the control (unmodified; solid black line), $\Delta g_o$ (Ball-Berry $g_o$ parameter adjusted; red line), $\Delta g_{night}$ (minimum nighttime threshold added; teal line), and $\Delta g_{min}$ (minimum conductance threshold added; blue line) simulations. Error bars corresponding to the observations (dashed) and each simulation (solid) are colored accordingly, and are calculated as +/- one standard deviation from the mean. Note that the simulations use meteorological forcings from an atmospheric dataset (see Methods), not the local meteorology from when the measurements were collected (some meteorological data was collected at the site, but not all variables required by the model). The simulated grid cell covers a much larger area than the observational data collection site.

505 **References**


506 Ball, J. T.: An Analysis of Stomatal Conductance, Stanford University., 1988.

507 Ball, J. T., Woodrow, I. E. and Berry, J. A.: A Model Predicting Stomatal
508 Conductance and its Contribution to the Control of Photosynthesis under
509 Different Environmental Conditions, in Progress in Photosynthesis Research,
510 edited by J. Biggins, pp. 221–224, Springer Netherlands. [online] Available from:
511 http://link.springer.com/chapter/10.1007/978-94-017-0519-6_48 (Accessed
512 27 April 2015), 1987.

513 Barnard, D. M. and Bauerle, W. L.: The implications of minimum stomatal
514 conductance on modeling water flux in forest canopies, J. Geophys. Res.-
515 Biogeosciences, 118(3), 1322–1333, doi:10.1002/jgrg.20112, 2013.

516 Bonan, G. B., Lawrence, P. J., Oleson, K. W., Levis, S., Jung, M., Reichstein, M.,
517 Lawrence, D. M. and Swenson, S. C.: Improving canopy processes in the
518 Community Land Model version 4 (CLM4) using global flux fields empirically
519 inferred from FLUXNET data, J. Geophys. Res.-Biogeosciences, 116, G02014,
520 doi:10.1029/2010JG001593, 2011.

521 Bonan, G. B., Oleson, K. W., Fisher, R. A., Lasslop, G. and Reichstein, M.:
522 Reconciling leaf physiological traits and canopy flux data: Use of the TRY and
523 FLUXNET databases in the Community Land Model version 4, J. Geophys. Res.-
524 Biogeosciences, 117, G02026, doi:10.1029/2011JG001913, 2012.

525 Bonan, G. B., Williams, M., Fisher, R. A. and Oleson, K. W.: Modeling stomatal
526 conductance in the earth system: linking leaf water-use efficiency and water
527 transport along the soil–plant–atmosphere continuum, Geosci Model Dev, 7(5),
528 2193–2222, doi:10.5194/gmd-7-2193-2014, 2014.

529 Bowden, J. D. and Bauerle, W. L.: Measuring and modeling the variation in
530 species-specific transpiration in temperate deciduous hardwoods, Tree Physiol.,
531 28(11), 1675–1683, 2008.

532 Caird, M. A., Richards, J. H. and Donovan, L. A.: Nighttime stomatal conductance
533 and transpiration in C-3 and C-4 plants, Plant Physiol., 143(1), 4–10,
534 doi:10.1104/pp.106.092940, 2007.

535 Collatz, G. J., Ball, J. T., Grivet, C. and Berry, J. A.: Physiological and environmental
536 regulation of stomatal conductance, photosynthesis and transpiration: a model
537 that includes a laminar boundary layer, Agric. For. Meteorol., 54(2–4), 107–136,
538 doi:10.1016/0168-1923(91)90002-8, 1991.

539 Dawson, T. E., Burgess S. S. O., Tu, K. P., Oliveira, R. S., Santiago, L. S., Fisher, J. B.,
540 Simonin, K. A., and Ambrose, A. R.: Nighttime transpiration in woody plants from
541 contrasting ecosystems. Tree Phys., 27**,** 561–575, 2007.

542 Dios, V. R. de, Turnbull, M. H., Barbour, M. M., Ontedhu, J., Ghannoum, O. and
543 Tissue, D. T.: Soil phosphorous and endogenous rhythms exert a larger impact

than CO2 or temperature on nocturnal stomatal conductance in Eucalyptus tereticornis, Tree Physiol., tpt091, doi:10.1093/treephys/tpt091, 2013.

Dirmeyer, P. A.: The terrestrial segment of soil moisture-climate coupling, Geophys. Res. Lett., 38, L16702, doi:10.1029/2011GL048268, 2011.

Fisher, J. B., Baldocchi, D. D., Misson, L., Dawson, T. E. and Goldstein, A. H.: What the towers don't see at night: nocturnal sap flow in trees and shrubs at two AmeriFlux sites in California, Tree Physiol., 27(4), 597–610, 2007.

Van Gorsel, E., Leuning, R., Cleugh, H. A., Keith, H., Kirschbaum, M. U. F. and Suni, T.: Application of an alternative method to derive reliable estimates of nighttime respiration from eddy covariance measurements in moderately complex topography, Agric. For. Meteorol., 148(6-7), 1174–1180, doi:10.1016/j.agrformet.2008.01.015, 2008.

Hetherington, A. M. and Woodward, F. I.: The role of stomata in sensing and driving environmental change, Nature, 424(6951), 901–908, doi:10.1038/nature01843, 2003.

Hirschi, M., Seneviratne, S. I., Alexandrov, V., Boberg, F., Boroneant, C., Christensen, O. B., Formayer, H., Orlowsky, B. and Stepanek, P.: Observational evidence for soil-moisture impact on hot extremes in southeastern Europe, Nat. Geosci., 4(1), 17–21, doi:10.1038/NGEO1032, 2011.

Kattge, J. and Knorr, W.: Temperature acclimation in a biochemical model of photosynthesis: a reanalysis of data from 36 species, Plant Cell Environ., 30(9), 1176–1190, doi:10.1111/j.1365-3040.2007.01690.x, 2007.

De Kauwe, M. G., Kala, J., Lin, Y.-S., Pitman, A. J., Medlyn, B. E., Duursma, R. A., Abramowitz, G., Wang, Y.-P. and Miralles, D. G.: A test of an optimal stomatal conductance scheme within the CABLE land surface model, Geosci Model Dev, 8(2), 431–452, doi:10.5194/gmd-8-431-2015, 2015.

Kirschbaum, M. U. F., Keith, H., Leuning, R., Cleugh, H. A., Jacobsen, K. L., van Gorsel, E. and Raison, R. J.: Modelling net ecosystem carbon and water exchange of a temperate Eucalyptus delegatensis forest using multiple constraints, Agric. For. Meteorol., 145(1-2), 48–68, doi:10.1016/j.agrformet.2007.04.002, 2007.

Lawrence, D. M., Oleson, K. W., Flanner, M. G., Thornton, P. E., Swenson, S. C., Lawrence, P. J., Zeng, X., Yang, Z.-L., Levis, S., Sakaguchi, K., Bonan, G. B. and Slater, A. G.: Parameterization Improvements and Functional and Structural Advances in Version 4 of the Community Land Model, J. Adv. Model. Earth Syst., 3, M03001, doi:10.1029/2011MS000045, 2011.

Leuning, R.: A critical appraisal of a combined stomatal-photosynthesis model for C3 plants, Plant Cell Environ., 18(4), 339–355, doi:10.1111/j.1365-3040.1995.tb00370.x, 1995.

Li, H., Huang, M., Wigmosta, M. S., Ke, Y., Coleman, A. M., Leung, L. R., Wang, A. and Ricciuto, D. M.: Evaluating runoff simulations from the Community Land Model

584 4.0 using observations from flux towers and a mountainous watershed, J.
585 Geophys. Res.-Atmospheres, 116, D24120, doi:10.1029/2011JD016276, 2011.

586 McLaughlin, S. B., Wullschleger, S. D., Sun, G. and Nosal, M.: Interactive effects of
587 ozone and climate on water use, soil moisture content and streamflow in a
588 southern Appalachian forest in the USA, New Phytol., 174(1), 125–136,
589 doi:10.1111/j.1469-8137.2007.01970.x, 2007.

590 Medlyn, B. E., Robinson, A. P., Clement, R. and McMurtrie, R. E.: On the validation
591 of models of forest CO2 exchange using eddy covariance data: some perils and
592 pitfalls, Tree Physiol., 25(7), 839–857, 2005.

593 Medlyn, B. E., Duursma, R. A., Eamus, D., Ellsworth, D. S., Prentice, I. C., Barton, C.
594 V. M., Crous, K. Y., De Angelis, P., Freeman, M. and Wingate, L.: Reconciling the
595 optimal and empirical approaches to modelling stomatal conductance, Glob.
596 Change Biol., 17(6), 2134–2144, doi:10.1111/j.1365-2486.2010.02375.x, 2011.

597 Miralles, D. G., Teuling, A. J., van Heerwaarden, C. C. and Vilà-Guerau de Arellano,
598 J.: Mega-heatwave temperatures due to combined soil desiccation and
599 atmospheric heat accumulation, Nat. Geosci., 7(5), 345–349,
600 doi:10.1038/ngeo2141, 2014.

601 Niyogi, D. S. and Raman, S.: Comparison of Four Different Stomatal Resistance
602 Schemes Using FIFE Observations, J. Appl. Meteorol., 36(7), 903–917,
603 doi:10.1175/1520-0450(1997)036<0903:COFDSR>2.0.CO;2, 1997.

604 Oleson, K. W., Lawrence, D. M., Bonan, G. B., Drewniak, B., Huang, M., Koven, C. D.,
605 Levis, S., Li, F., Riley, W. J., Subin, Z. M., Swenson, S. C., Thornton, P. E., Bozbiyik,
606 A., Fisher, R. A., Kluzek, E., Lamarque, J.-F., Lawrence, P. J., Leung, L. R., Lipscomb,
607 W., Muszala, S., Ricciuto, D. M., Sacks, W. J., Sun, Y., Tang, J. Y. and Yang, Z.-L.:
608 Technical Description of version 4.5 of the Community Land Model (CLM), NCAR
609 Tech. Note, NCAR/TN-503+STR, doi:10.5065/D6RR1W7M, 2013.

610 Phillips, N. G., Lewis, J. D., Logan, B. A. and Tissue, D. T.: Inter- and intra-specific
611 variation in nocturnal water transport in Eucalyptus, Tree Physiol., 30(5), 586–
612 596, doi:10.1093/treephys/tpq009, 2010.

613 Scholz, F. G., Bucci, S. J., Goldstein, G., Meinzer, F. C., Franco, A. C. and Miralles-
614 Wilhelm, F.: Removal of nutrient limitations by long-term fertilization decreases
615 nocturnal water loss in savanna trees, Tree Physiol., 27(4), 551–559,
616 doi:10.1093/treephys/27.4.551, 2007.

617 Sellers, P. j., Randall, D. a., Collatz, G. j., Berry, J. a., Field, C. b., Dazlich, D. a., Zhang,
618 C., Collelo, G. d. and Bounoua, L.: A Revised Land Surface Parameterization (SiB2)
619 for Atmospheric GCMS. Part I: Model Formulation, J. Clim., 9(4), 676–705,
620 doi:10.1175/1520-0442(1996)009<0676:ARLSPF>2.0.CO;2, 1996.

621 Wei, J. and Dirmeyer, P. A.: Dissecting soil moisture-precipitation coupling,
622 Geophys. Res. Lett., 39, L19711, doi:10.1029/2012GL053038, 2012.

623 Zeppel, M. J. B., Lewis, J. D., Phillips, N. G. and Tissue, D. T.: Consequences of
624 nocturnal water loss: a synthesis of regulating factors and implications for
625 capacitance, embolism and use in models, Tree Physiol., 34(10), 1047–1055,
626 doi:10.1093/treephys/tpu089, 2014.

627

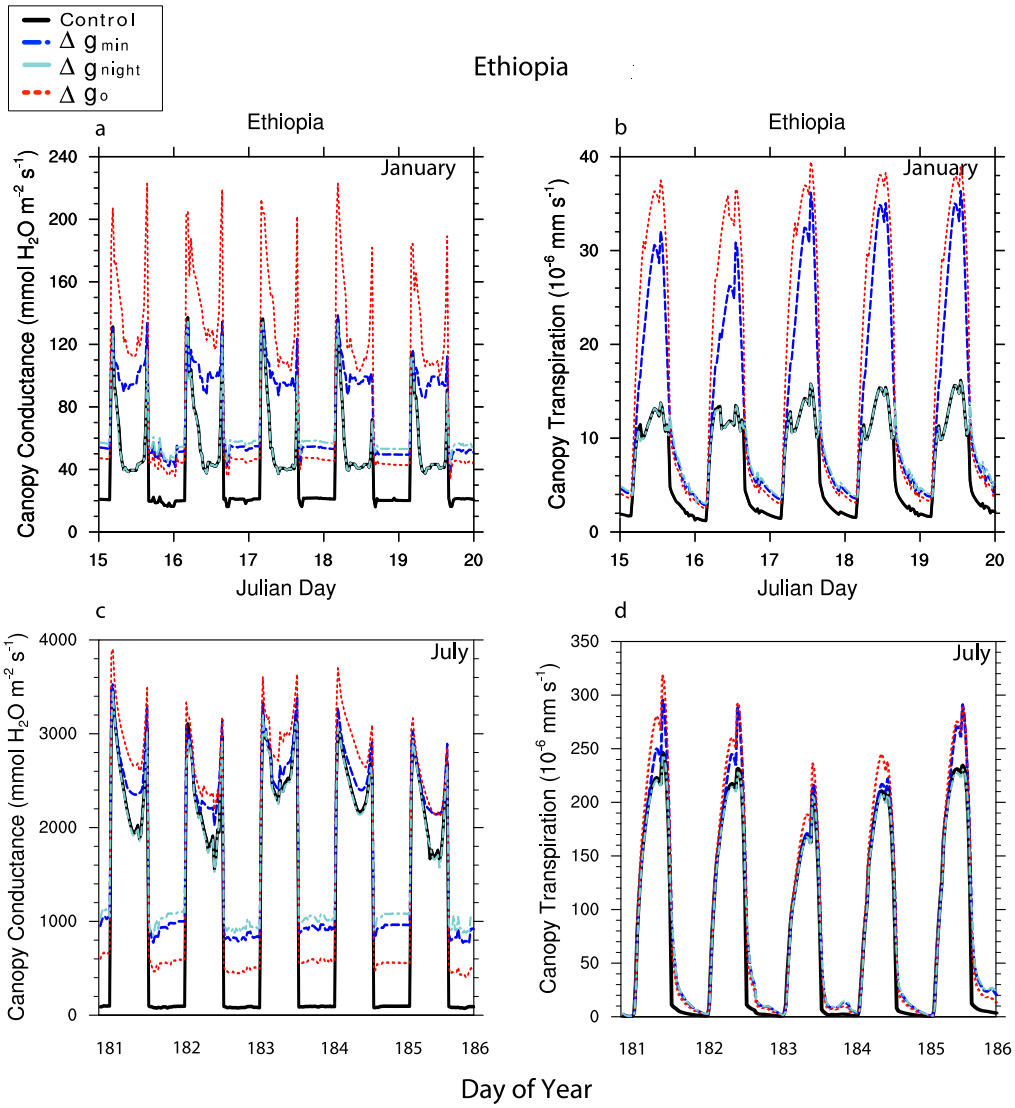


628
629

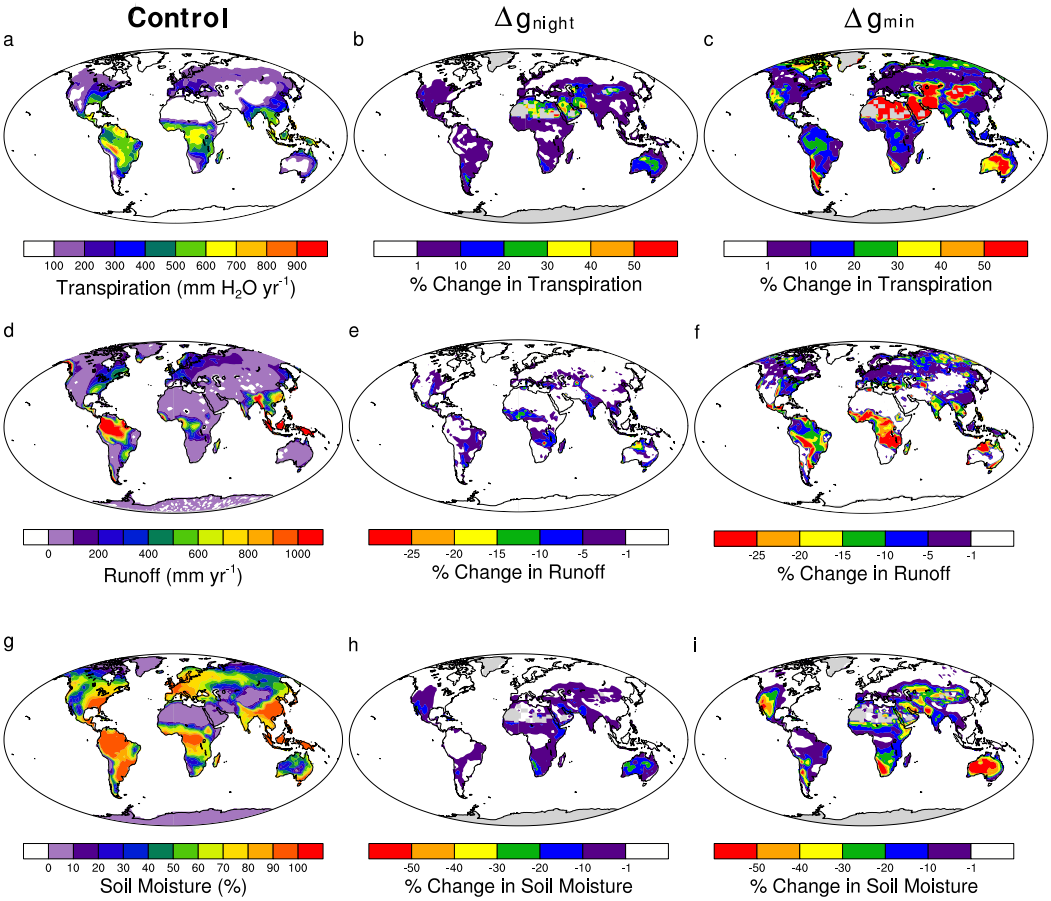
Control
Δgnight
Δgmin
a
b
c
100 200 300 400 500 600 700 800 900
Transpiration (mm H2O yr-1)
1 10 20 30 40 50
% Change in Transpiration
1 10 20 30 40 50
% Change in Transpiration
d
e
f
0 200 400 600 800 1000
Runoff (mm yr-1)
-25 -20 -15 -10 -5 -1
% Change in Runoff
-25 -20 -15 -10 -5 -1
% Change in Runoff
g
h
i
0 10 20 30 40 50 60 70 80 90 100
Soil Moisture (%)
-50 -40 -30 -20 -10 -1
% Change in Soil Moisture
-50 -40 -30 -20 -10 -1
% Change in Soil Moisture

630

631

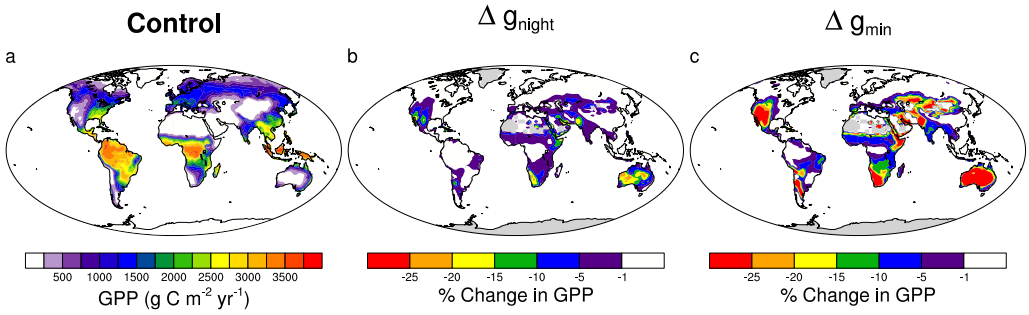
Control
Δ g night
Δ g min
a
b
c
500 1000 1500 2000 2500 3000 3500
GPP (g C m-2 yr-1)
-25 -20 -15 -10 -5 -1
% Change in GPP
-25 -20 -15 -10 -5 -1
% Change in GPP

632

633

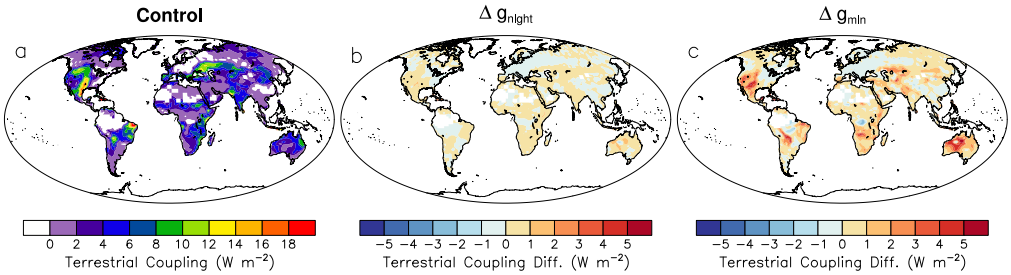
Control
a
0 2 4 6 8 10 12 14 16 18
Terrestrial Coupling (W m−2)
Δ gnlght
b
−5 −4 −3 −2 −1 0 1 2 3 4 5
Terrestrial Coupling Diff. (W m−2)
Δ gmln
c
−5 −4 −3 −2 −1 0 1 2 3 4 5
Terrestrial Coupling Diff. (W m−2)

634

635

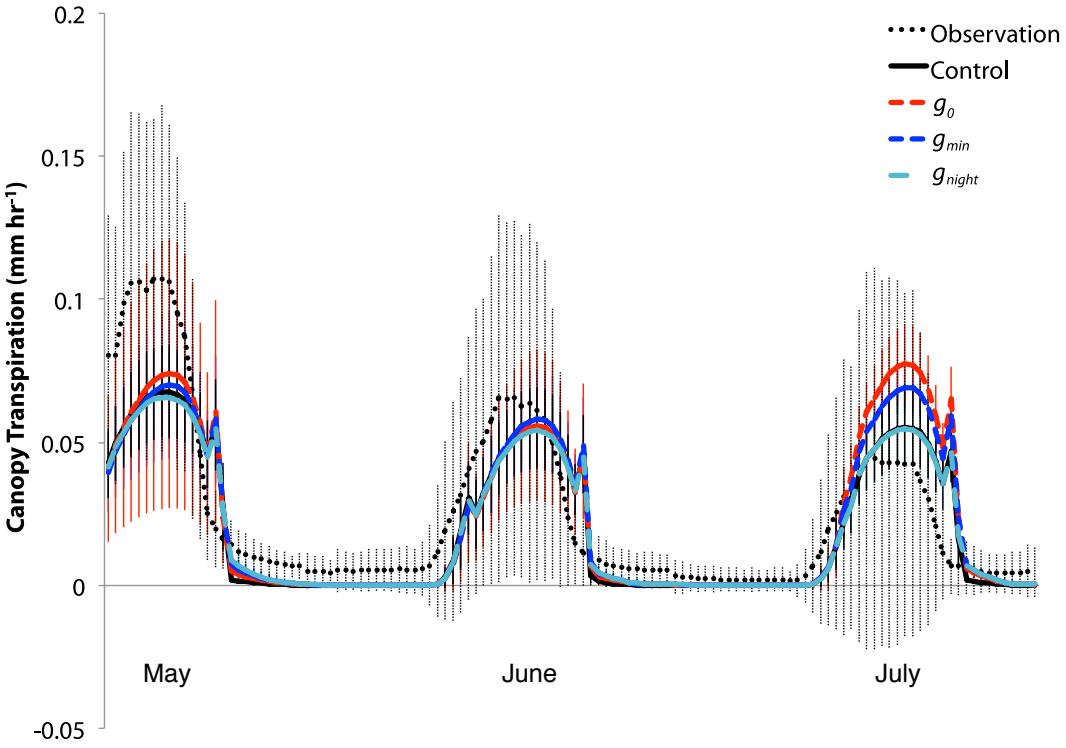
0.2
0.15
0.1
0.05
0
-0.05
Canopy Transpiration (mm hr-1)
May
June
July
Observation
Control
g0
gmin
gnight

636